

 Open access • Journal Article • DOI:10.1109/TNSRE.2009.2033061

Path Control: A Method for Patient-Cooperative Robot-Aided Gait Rehabilitation

— [Source link](#) 

Alexander Duschau-Wicke, J. von Zitzewitz, Andrea Caprez, Lars Lünenburger ...+1 more authors

Institutions: ETH Zurich

Published on: 01 Feb 2010 - International Conference of the IEEE Engineering in Medicine and Biology Society

Topics: Rehabilitation robotics, Gait (human) and Gait analysis

Related papers:

- [Patient-cooperative strategies for robot-aided treadmill training: first experimental results](#)
- [Robot Assisted Gait Training With Active Leg Exoskeleton \(ALEX\)](#)
- [Design and Evaluation of the LOPES Exoskeleton Robot for Interactive Gait Rehabilitation](#)
- [Treadmill training of paraplegic patients using a robotic orthosis](#)
- [Review of control strategies for robotic movement training after neurologic injury](#)

Share this paper:    

View more about this paper here: <https://typeset.io/papers/path-control-a-method-for-patient-cooperative-robot-aided-acidavy48e>



University of Zurich
Zurich Open Repository and Archive

Winterthurerstr. 190
CH-8057 Zurich
<http://www.zora.uzh.ch>

Year: 2010

Path control: a method for patient-cooperative robot-aided gait rehabilitation

Duschau-Wicke, A; von Zitzewitz, J; Caprez, A; Lunenburger, L; Riener, R

Duschau-Wicke, A; von Zitzewitz, J; Caprez, A; Lunenburger, L; Riener, R (2010). Path control: a method for patient-cooperative robot-aided gait rehabilitation. IEEE transactions on neural systems and rehabilitation engineering : a publication of the IEEE Engineering in Medicine and Biology Society, 18(1):38-48.

Postprint available at:
<http://www.zora.uzh.ch>

Posted at the Zurich Open Repository and Archive, University of Zurich.
<http://www.zora.uzh.ch>

Originally published at:
IEEE transactions on neural systems and rehabilitation engineering : a publication of the IEEE Engineering in Medicine and Biology Society 2010, 18(1):38-48.

Path Control: A Method for Patient-Cooperative Robot-Aided Gait Rehabilitation

Alexander Duschau-Wicke, *Graduate Student Member, IEEE*,

Joachim von Zitzewitz, *Graduate Student Member, IEEE*, Andrea Caprez, Lars Lünenburger, *Member, IEEE*,
and Robert Riener, *Member, IEEE*

Abstract—Gait rehabilitation robots are of increasing importance in neurorehabilitation. Conventional devices are often criticized because they are limited to reproducing predefined movement patterns. Research on patient-cooperative control strategies aims at improving robotic behavior. Robots should support patients only as much as needed and stimulate them to produce maximal voluntary efforts. This paper presents a patient-cooperative strategy that allows patients to influence the timing of their leg movements along a physiologically meaningful path. In this “path control” strategy, compliant virtual walls keep the patient’s legs within a “tunnel” around the desired spatial path. Additional supportive torques enable patients to move along the path with reduced effort. Graphical feedback provides visual training instructions. The path control strategy was evaluated with 10 healthy subjects and 15 subjects with incomplete spinal cord injury. The spatio-temporal characteristics of recorded kinematic data showed that subjects walked with larger temporal variability with the new strategy. Electromyographic data indicated that subjects were training more actively. A majority of iSCI subjects was able to actively control their gait timing. Thus, the strategy allows patients to train walking while being helped rather than controlled by the robot.

Index Terms—Control, gait rehabilitation, patient-cooperative, rehabilitation robotics.

I. INTRODUCTION

FUNCTIONAL, task-oriented training plays an important role in neurorehabilitation today. In particular, body-weight supported treadmill training is successfully ap-

plied to the rehabilitation of patients with neurological gait disorders after stroke [1] or incomplete spinal cord injury (iSCI) [2].

However, this kind of training is strenuous and physically demanding for therapists; thus, it is usually limited by personnel shortage and fatigue of the therapist. Therefore, several robotic devices have been developed to overcome these deficiencies. The first generation of these devices has been in clinical use for several years: the Lokomat (Hocoma AG, Switzerland) [3], the ReoAmbulator (Motorika, USA), and the Gait Trainer (Reha-Stim, Germany) [4].

Originally, these devices only moved the patient along predefined, fixed trajectories and did not adapt their movements to the activity of the patient. This kind of *position-controlled* training is well suited for patients who are in the early phase of rehabilitation or severely affected. However, the strong guidance of the robot does not provide an ideal training ground for patients capable of (some) voluntary motor control. If patients are allowed to remain completely passive, they tend to train with reduced activity of muscles and metabolism [5]. On the other hand, if patients are motivated to walk actively, they work against the resistance of the device, which results in abnormal muscle activity patterns [6].

To resolve these shortcomings, *patient-cooperative* control strategies are being developed by numerous research groups [7]–[16]. These strategies aim at empowering patients to influence their movements, while still providing sufficient *guidance* and *support* to ensure successful walking. When patients can move more freely, changes in muscle activation are reflected in the walking pattern. This experience can cause a consistent feeling of success, which is hypothesized to increase motivation. Variations in muscle activation would be directly causing consistent afferent feedback variations that retrain the neural networks in brain and spinal cord. This feedback can challenge the nervous system and lead to favorable training effects in iSCI and hemiparetic patients [17], [18].

First efforts towards patient-cooperativeness concentrated on adding *compliance* to the devices. For example, the Lokomat was augmented with impedance control and adaptive control algorithms [9]. Moreover, new devices with inherently more compliant features have been developed, such as the pneumatic PAM and POGO devices of University of California, Irvine [19], or the LOPES exoskeleton of Universiteit Twente [20].

The prevailing paradigm for supporting patients is the concept of “assist as needed” (AAN) [8], [10]. In order to stimulate maximal voluntary contribution of the patient, robotic devices are supposed to reduce their supportive actions to a min-

Manuscript received December 10, 2008; revised June 18, 2009; accepted August 27, 2009. First published October 06, 2009; current version published February 24, 2010. This work was supported by the National Institute on Disability and Rehabilitation Research (NIDRR) under Grant H133E070013.

A. Duschau-Wicke is with the Sensory-Motor Systems Lab, Institute of Robotics and Intelligent Systems, Department of Mechanical and Process Engineering, ETH Zurich, 8092 Zurich, Switzerland, and also with the Spinal Cord Injury Center, University Hospital Balgrist, University of Zurich, 8008 Zurich, Switzerland, and also with the Hocoma AG, 8604 Volketswil, Switzerland (e-mail: duschau@mavt.ethz.ch).

J. v. Zitzewitz and R. Riener are with the Sensory-Motor Systems Lab, Institute of Robotics and Intelligent Systems, Department of Mechanical and Process Engineering, ETH Zurich, 8092 Zurich, Switzerland, and also with the Spinal Cord Injury Center, University Hospital Balgrist, University of Zurich, 8008 Zurich, Switzerland (e-mail: zitzewitz@mavt.ethz.ch; riener@mavt.ethz.ch).

A. Caprez is with the Sensory-Motor Systems Lab, Institute of Robotics and Intelligent Systems, Department of Mechanical and Process Engineering, ETH Zurich, 8092 Zurich, Switzerland, and also with the Spinal Cord Injury Center, University Hospital Balgrist, University of Zurich, 8008 Zurich, Switzerland, and also with the Institute for Biomechanics, ETH Zurich, 8092 Zurich, Switzerland (e-mail: acaprez@student.ethz.ch).

L. Lünenburger is with Hocoma AG, 8604 Volketswil, Switzerland (e-mail: lars.luenenburger@hocoma.com).

Digital Object Identifier 10.1109/TNSRE.2009.2033061

imum. This minimal support needs to be sufficient to allow patients to complete the desired task in a physiologically correct way. However, all approaches using classical impedance control share the disadvantage of imposing a defined timing of movements on the patient. As spatial and temporal corrections are coupled in these control strategies, it is not possible to achieve freedom in timing without losing guidance in space. If the impedance setting is too stiff, patients feel passively moved; if it is too soft, patients are not corrected in space and might move in undesired patterns.

A solution to this problem was first proposed for the upper extremity robot MIT-MANUS [21]. The controller of the robot simulated a virtual tunnel in space. Patients could autonomously move their hands through this tunnel. If they did not move forward as desired, the moving “back wall” of this tunnel carried their hand along after a certain amount of time. Cai *et al.* [11] applied two similar concepts to spinalized mice using a miniature rehabilitation robot. Firstly, they created a virtual tunnel similar to the approach for the MIT-MANUS, but without a moving “back wall.” The mice could move their hind limb freely within this tunnel while walking on a treadmill. Secondly, they trained the mice with a “moving window” that allowed some freedom, but kept them synchronized to the treadmill. Mice trained with the “moving window” approach improved faster than those trained with a classical position control strategy. Banala *et al.* [13] implemented the virtual tunnel approach of Cai *et al.* [11] for their “Active Leg Exoskeleton” (ALEX) and tested the approach with healthy and stroke subjects.

Likewise motivated by the work of Cai *et al.* [11], we developed a similar approach for the Lokomat [12]. However, to focus more on leg postures than on end-effector position, we designed a torque field tunnel in joint space rather than a force field in Cartesian space. Pilot studies indicated that training of iSCI subjects requires more control over the amount of freedom provided by the controller than training of healthy subjects. The iSCI subjects could not cope with the freedom of timing that was possible in a plain virtual tunnel. Consequently, we superposed the “moving window” approach and the virtual tunnel from Cai *et al.* [11] to one control strategy. The moving window restricts the domain of possible leg postures to a region within the virtual tunnel. The window size determines how much freedom in timing the subjects experience within the tunnel.

As our algorithm allows subjects to move actively along the spatial *path* of a defined walking pattern, it is referred to as “path control.” The additional freedom provided by this patient-cooperative control strategy is combined with a training task, in which patients have to autonomously control their legs within the given freedom. A visual display shows both the patients’ movements and the reference movements, which the patients are supposed to track (Fig. 1).

We evaluated the patient-cooperative strategy with respect to the following research questions. 1) Does the path control strategy allow subjects to influence the timing of their movements? 2) Does training with the path control strategy result in more active participation of subjects? 3) Can we modulate how actively subjects participate in the training by adjusting the support? 4) Are iSCI subjects able to perform gait training with the path control strategy?



Fig. 1. Healthy subject training in the Lokomat with the path control strategy.

II. MATERIALS AND METHODS

A. Gait Training Robot

Experiments were performed with the gait rehabilitation robot Lokomat. The robot automates body weight-supported treadmill training of patients with locomotor dysfunctions in the lower extremities such as spinal cord injury and hemiplegia after stroke [3]. It comprises two actuated leg orthoses that are attached to the patient’s legs. Each orthosis has one linear drive in the hip joint and one in the knee joint to induce flexion and extension movements of hip and knee in the sagittal plane. Knee and hip joint torques can be determined from force sensors between actuators and orthosis. Passive foot lifters can be added to induce ankle dorsiflexion during swing phase. A body weight support system relieves patients from a definable amount of their body weight via a harness.

B. Path Control Algorithm

Existing position and impedance control algorithms of the Lokomat [9] define a reference trajectory $\mathbf{q}_{\text{ref}}(S)$ for each leg.¹ The variable S denotes the relative position in the gait cycle, which is normalized to the interval $[0, 1)$. Two subsequent heel strikes of the same foot define the beginning ($S = 0$) and end ($S \rightarrow 1$) of a step. S is calculated by applying the modulo operation with respect to 1 (mod 1) to the product of the time t and the desired replay speed v_{replay}

$$S(t) = (v_{\text{replay}} \cdot t) \bmod 1. \quad (1)$$

The reference trajectory $\mathbf{q}_{\text{ref}}(S)$ has been recorded from healthy subjects [3] and is used as set point for the impedance controller. The replay speed v_{replay} is a function of the treadmill speed v_{TM} chosen by the therapist

$$v_{\text{replay}} = v_{\text{TM}}/c_{\text{pat}}. \quad (2)$$

¹The following notation is used throughout this paper: all vectors of joint angles and torques consist of two elements, the first one for the hip joint and the second one for the knee joint, e.g., $\mathbf{q} = (q^{(1)}, q^{(2)})^T = (q_{\text{hip}}, q_{\text{knee}})^T$. The control algorithms discussed in this paper are always defined for a single leg. The second leg is controlled by an independent second instance of the respective control algorithm.

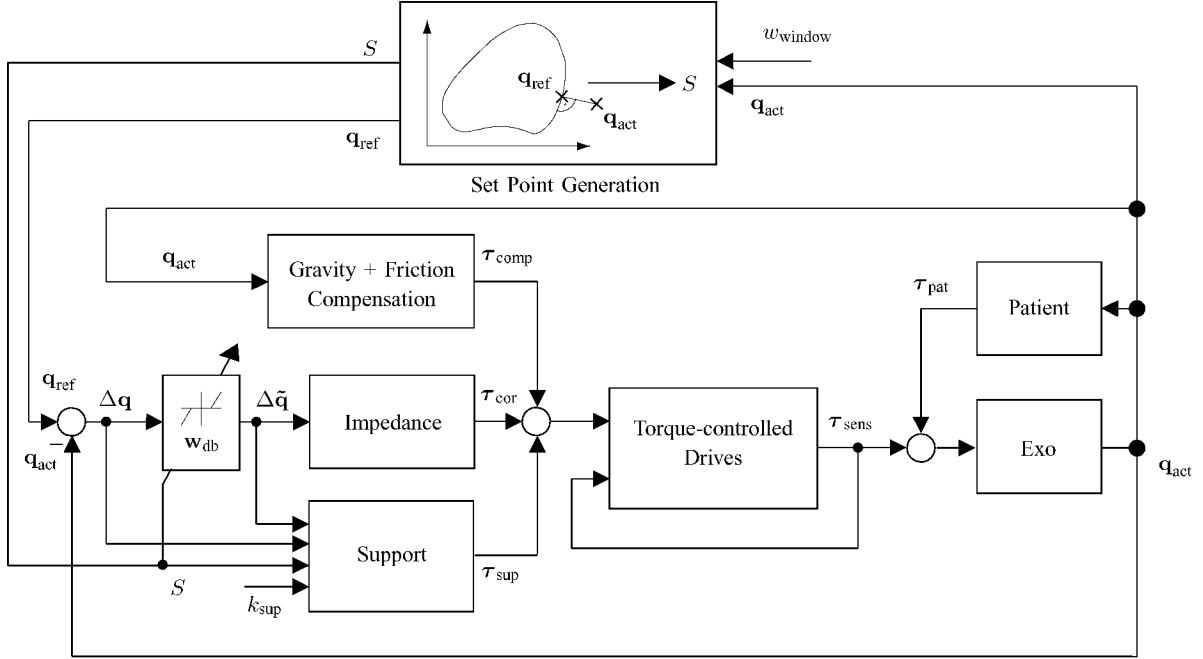


Fig. 2. Block diagram of path control strategy. The “Set Point Generation” block determines the relative position S in the gait cycle [(3), (13), and (14)]. The “Gravity + Friction Compensation” block computes the torques τ_{comp} based on a model of the Lokomat [9]. The corrective torques τ_{cor} of the “Impedance” block keep the subject’s leg within the tunnel [(9)]. The “Support” block computes the supportive torques τ_{sup} [(10) and (11)]. The “torque-controlled drives” apply the desired torques to the Lokomat exoskeleton (“Exo”). These torques are measured as τ_{sens} . Together with the patient’s torques τ_{pat} , they move the exoskeleton and determine the actual angles \mathbf{q}_{act} .

The parameter c_{pat} synchronizes Lokomat and treadmill. It can either be set manually by the therapist or automatically by an iterative learning algorithm [22].

For the path control algorithm, S is not calculated as a function of time, but as a function of the actual joint angles \mathbf{q}_{act} (Fig. 2). A dynamic *set point generation* algorithm chooses S such that the Euclidean distance between $\mathbf{q}_{\text{ref}}(S)$ and \mathbf{q}_{act} is minimized

$$S : \|\mathbf{q}_{\text{ref}}(S) - \mathbf{q}_{\text{act}}\|^2 \stackrel{!}{=} \min. \quad (3)$$

An adjustable dead band of width $w_{\text{db}}(S)$ creates a virtual tunnel around the reference trajectory. The width of the dead band has been designed heuristically based on the experience from pretrials. It was shaped in a way that allows more spatial variation during late swing and early stance phase to account for the large variability of knee flexion at heels strike of our test subjects. Additionally, the reference trajectory \mathbf{q}_{ref} has been adapted to a less pronounced loading response and more knee flexion during swing phase so that the desired dead band spreads symmetrically around the reference. This way, a common tunnel was obtained that could be used for all subjects (Fig. 3). Within the tunnel, the controller is in so called “free-run” mode, i.e., the output τ_{cor} of the impedance is zero, and gravity and friction torques of the robot are compensated (Fig. 2). Therefore, subjects can move freely and with their own timing as long as they stay within the tunnel. Leg postures outside the tunnel are corrected by the impedance controller. The spring constant \mathbf{K} of the virtual impedance is chosen as a function of the distance $\Delta\tilde{\mathbf{q}}$ to the tunnel wall

$$\Delta\mathbf{q} = \mathbf{q}_{\text{ref}}(S) - \mathbf{q}_{\text{act}} \quad (4)$$

$$\Delta\tilde{\mathbf{q}}^{(i)} = \begin{cases} \Delta q^{(i)} - \frac{1}{2}w_{\text{db}}^{(i)}, & \Delta q^{(i)} > \frac{1}{2}w_{\text{db}}^{(i)} \\ \Delta q^{(i)} + \frac{1}{2}w_{\text{db}}^{(i)}, & \Delta q^{(i)} < -\frac{1}{2}w_{\text{db}}^{(i)} \\ 0, & |\Delta q^{(i)}| \leq \frac{1}{2}w_{\text{db}}^{(i)} \end{cases} \quad (5)$$

$$\tilde{K}^{(i)} = c_K^{(i)} \|\Delta\tilde{\mathbf{q}}\|^2 \quad (6)$$

$$K^{(i)} = \min(\tilde{K}^{(i)}, K_{\text{max}}^{(i)}) \quad (7)$$

$$\mathbf{K} = \begin{pmatrix} K^{(1)} & 0 \\ 0 & K^{(2)} \end{pmatrix} \quad (8)$$

where $c_K^{(i)}$ are constants which were determined by trial and error, such that the wall of the tunnel felt comfortably soft for subjects ($c_K^{(1)} = 72000 \text{ Nm/rad}^2$, $c_K^{(2)} = 54000 \text{ Nm/rad}^2$). The stiffness was chosen to be nonlinear to allow for a compromise between soft contact with the wall and strong corrections for larger deviations. The constants $K_{\text{max}}^{(i)}$ are the element-wise upper limits for \mathbf{K} ($K_{\text{max}}^{(1)} = 720 \text{ Nm/rad}$, $K_{\text{max}}^{(2)} = 540 \text{ Nm/rad}$), which prevent the controller from becoming too stiff for large angular deviations $\Delta\mathbf{q}$. An additional damping constant \mathbf{B} is in turn determined as a function of \mathbf{K} such that the system is critically damped ($B^{(1)} = 2\sqrt{K^{(1)}}$, $B^{(2)} = 1.5\sqrt{K^{(2)}}$) as for the Lokomat impedance controller described in [9].

The output of the virtual impedance is calculated as

$$\tau_{\text{cor}} = \mathbf{K}\Delta\tilde{\mathbf{q}} + \mathbf{B}\frac{d}{dt}\Delta\tilde{\mathbf{q}}. \quad (9)$$

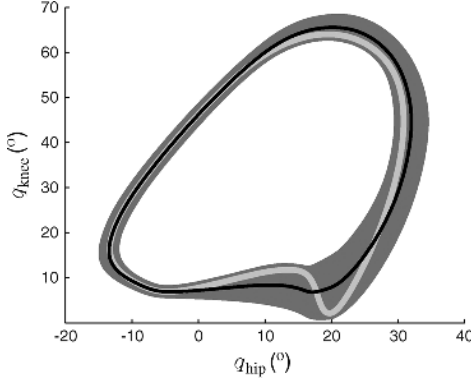


Fig. 3. Virtual tunnel around the reference path in joint space. The light grey line shows the original Lokomat reference pattern as used for the POS condition. The black line displays the adapted reference trajectory $\mathbf{q}_{\text{ref}}(S)$ as it was applied for the path control strategy. The dark grey area displays the extent of the virtual tunnel, as defined by \mathbf{w}_{db} . The virtual tunnel has been designed to allow increased spatial variation during late swing and early stance phase.

Adjustable supportive torques can be superimposed to the controller output. To determine the direction of support, a torque vector is calculated by differentiating the reference trajectory \mathbf{q}_{ref} with respect to the relative position in the gait cycle S . Thus, the direction of the torque vector is tangential to the movement path in joint space

$$\tilde{\boldsymbol{\tau}}_{\text{sup}}(S) = \frac{d}{dS} \mathbf{q}_{\text{ref}}(S). \quad (10)$$

To avoid interferences between the torques $\boldsymbol{\tau}_{\text{cor}}$ and the supportive torques, we scale the support as a linear function of the distance to the center of the path. The actual supportive torques are

$$\boldsymbol{\tau}_{\text{sup}}(S) = \frac{\tilde{\boldsymbol{\tau}}_{\text{sup}}(S)}{\|\tilde{\boldsymbol{\tau}}_{\text{sup}}\|} \cdot (1 - d_{\text{center}}) \cdot k_{\text{sup}} \quad (11)$$

where k_{sup} is a scalar factor that determines the amount of support, and

$$d_{\text{center}} = \frac{\|\Delta \mathbf{q}\| - \|\Delta \tilde{\mathbf{q}}\|}{\|\mathbf{w}_{\text{db}}\|}, \quad d_{\text{center}} \in (0, 1) \quad (12)$$

is the relative distance to the center of the path. Thus, supportive torques are only provided within the tunnel, i.e., when $\|\Delta \tilde{\mathbf{q}}\| = 0$.

The supportive torques are not only important for helping a patient to overcome weaknesses. They also reduce the effect of the uncompensated inertia of the robot. In preliminary experiments, a support gain k_{sup} of 5–7 Nm was required by healthy subjects for comfortable walking. The support gain can be adjusted by the therapist during the training.

An optional “moving window” limits free movements to a region of the tunnel. The window moves with v_{replay} , which is determined according to (2). The synchronization factor c_{pat} is adjusted automatically as described in [22]. During stance phase, the velocity of the treadmill and the progression speed of the patient’s leg always match, because the patient’s leg is propelled by the treadmill. However, during swing phase, the patient can move faster or slower than v_{replay} . If he or she moves

constantly faster than v_{replay} , the patient will finally approach the compliant “front wall” of the window. Consequently, he or she will be slowed down to v_{replay} . If the patient moves slower than v_{replay} , he or she will reach the compliant “back wall” and will be pushed forward by the robot. In case of an active moving window, (3) is augmented with these inequality constraints for S

$$S \leq (v_{\text{replay}} \cdot t + w_{\text{window}}) \bmod 1 \quad (13)$$

$$S \geq (v_{\text{replay}} \cdot t - w_{\text{window}}) \bmod 1 \quad (14)$$

where w_{window} is the definable width from the window center to its back and front walls. Thus, the back and front walls of the moving window are rendered by the virtual impedance in the same way as the tunnel wall according to (9).

C. Training Task

A visual display presents both task instructions and performance feedback to the patient. This visual feedback provides a so-called “virtual mirror” [23] comprising a 3-D, virtual representation (avatar) of the patient on a 3×2 m projection screen (Fig. 1). The movements of this avatar represent the movements of the patient. A second pair of semi-transparent legs (“ghost legs”) indicates the reference movements. The reference movements are based on the reference trajectory $\mathbf{q}_{\text{ref}}(S_{\text{replay}}(t))$, where $S_{\text{replay}}(t)$ refers to $S(t)$ calculated according to (1).

Patients are instructed to match the movements of their “mirror legs” with the movements of the “ghost legs.” The timing error $\Delta S(t)$ is defined as follows:

$$\Delta S(t) = (v_{\text{replay}} \cdot t) \bmod 1 - S_{\text{path}}(t) \quad (15)$$

where $S_{\text{path}}(t)$ is the value of S calculated by (3) at time t . By matching the shown reference movements, the patient minimizes ΔS . Thus, ΔS can be used as a measure of the patient’s performance in the training task.

D. Experimental Design

Two experiments were conducted to evaluate the path control strategy. In a first experiment, the possibility to influence the timing of walking and the effects of different levels of support on muscle activity were assessed on healthy subjects. In a second experiment, iSCI subjects performed the training task to judge its feasibility. All experimental procedures were approved by the Ethics Committee of the Canton of Zurich, Switzerland, and all participants provided informed consent before the experiments.

1) *Experiment With Healthy Subjects:* Ten healthy young adults (7 male, 3 female; mean age 26.3 years, range 19–34 years) volunteered for the experiment.

Prior to the experiment, surface EMG electrodes were attached to the subjects’ gastrocnemius medialis (GM), tibialis anterior (TA), vastus medialis (VM), rectus femoris (RF), and biceps femoris (BF) muscles of the left leg. The electrodes were placed according to the SENIAM guidelines [24]. Custom-built foot-switches were taped under the heel of the left foot of the subjects to determine heel strikes.

TABLE I
PATIENT CHARACTERISTICS

Subj. No.	Sex	Age (y)	Lev. of injury	AIS	SCIM (mob.)	WISCI (mob.)	k_{sup} (Nm)
P1	m	31	L2	A	11	12	6
P2	m	42	L2	D	18	19	n/a
P3	m	63	L4	D	26	20	5
P4	f	63	T9	D	29	20	5
P5	f	41	Th9	C	27	18	6
P6	m	63	L3	B	10	16	6
P7	m	51	Th9	C	10	5	7
P8	m	35	C7	D	23	20	5
P9	m	33	L3	B	23	18	6
P10	f	62	L3	D	27	20	4
P11	m	53	L4	A	11	16	5
P12	f	64	L3	C	15	16	6
P13	m	31	L1	C	14	12	5
P14	f	53	L3	D	15	20	5
P15	m	61	C4	D	17	15	2

iSCI subjects were classified according to the ASIA Impairment Scale (AIS) [25]. The capabilities of the iSCI subjects were assessed with the mobility subscore of the SCIM III questionnaire [26], which can range from 0 to 30, and with the WISCI II score [27], which can range from 0 to 20. For both scores, higher values indicate better mobility.

Subjects walked with the Lokomat under five different conditions: 1) POS: position control with the Lokomat controller set to maximum stiffness ($K^{(1)} = 1200$ Nm/rad, $K^{(2)} = 900$ Nm/rad), replaying $\mathbf{q}_{\text{ref}}(S_{\text{replay}}(t))$, 2) PATHLOW: path control with low support ($k_{\text{sup}} = 5$ Nm), 3) PATHMEDIUM: path control with medium support ($k_{\text{sup}} = 7$ Nm), 4) PATHHIGH: path control with high support ($k_{\text{sup}} = 10$ Nm), and 5) ZEROIMP: zero impedance control with gravity and friction torques of the Lokomat compensated. Under all path control conditions, w_{window} was set to 20% of the gait cycle. The visual feedback was always presented to the subjects, who were instructed to walk actively and match the shown movements. However, under condition POS, the task was trivial, as the position controller of the Lokomat ensured near to perfect tracking. The order of the conditions was randomized. Subjects were unloaded with 30% of their body weight to obtain similar conditions as in typical training of iSCI subjects.

Under each condition, data was recorded for one minute after an acclimation phase of two minutes. In addition to the EMG signals, joint angles from the left hip and knee joints were recorded by sensors at the joint axes of the Lokomat.

2) *Experiment With iSCI Subjects*: 15 chronic iSCI subjects (Table I) walked with the Lokomat under three different conditions: 1) position control, 2) impedance control with the Lokomat controller set to 40% of the maximum stiffness, and 3) path control with w_{window} set to 20% of the gait cycle and the support gain k_{sup} adjusted individually for each patient (Table I). The therapist was instructed to adjust k_{sup} to the minimal value that enabled the patient to walk in the path control mode. Again, visual feedback was presented to the subjects under all conditions, and the subjects were instructed to match the displayed movements of the “ghost legs.” The order of the conditions was randomized. Subjects were unloaded with 30%–50% of their body weight.

During walking under the path control condition, the timing error $\Delta S(t)$ was recorded as a quantitative measure how well the subjects could accomplish the training task.

E. Data Analysis

1) *Experiment With Healthy Subjects*: To quantify the amount of temporal and spatial variations in the gait patterns during walking in the different conditions, we computed the spatio-temporal characteristics of the recorded trajectories $\mathbf{q}_{\text{act}}(t)$ according to the procedure described by Ilg *et al.*[28].

The recorded joint angles of each condition were cut into single strides triggered by the heel strike signal of the foot switches. The single strides were normalized in time to the interval $[0, 1]$. The trajectory of the k th normalized stride is referred to as $\mathbf{q}^{(k)}(S)$, and the number of recorded strides is denoted N . The average trajectory $\mathbf{q}_{\text{avg}}(S)$ was determined as a reference for the spatio-temporal analysis

$$\mathbf{q}_{\text{avg}}(S) = \frac{1}{N} \sum_{k=1}^N \mathbf{q}^{(k)}(S). \quad (16)$$

Each trajectory $\mathbf{q}^{(k)}$ was mapped to the reference trajectory \mathbf{q}_{avg} by a spatial shift function $\boldsymbol{\xi}^{(k)}(S)$ and a time shift function $\tau_{\text{shift}}^{(k)}(S)$

$$\mathbf{q}^{(k)}(S) = \mathbf{q}_{\text{avg}}\left(S + \tau_{\text{shift}}^{(k)}(S)\right) + \boldsymbol{\xi}^{(k)}(S). \quad (17)$$

The values of the shift functions $\boldsymbol{\xi}^{(k)}(S)$ and $\tau_{\text{shift}}^{(k)}(S)$ were determined by optimization as described in [29]. The weighting factor for the optimization was determined according to the rules for human movement data suggested in [28].

Finally, the spatial variability var_{ξ} and the temporal variability var_{τ} as defined in [28] were computed using the following equations:

$$\text{var}_{\xi} = \frac{1}{N} \sum_{k=1}^N \left(\int_0^1 \left| \boldsymbol{\xi}^{(k)}(S) \right| dS \right) \quad (18)$$

$$\text{var}_{\tau} = \frac{1}{N} \sum_{k=1}^N \left(\int_0^1 \left| \tau_{\text{shift}}^{(k)}(S) \right| dS \right). \quad (19)$$

The resulting spatial and temporal variability were compared by a Kruskal–Wallis nonparametric ANOVA at the 5% significance level [30]. Multiple comparisons were accounted for by the Tukey–Kramer adjustment.

To better understand the interactions between robot and subject, the interaction torques in the joints of the robot have been calculated. The robot’s force sensors are located between drives and exoskeleton and not directly at the interaction points with the human, such that a model of the exoskeleton’s dynamics has to be used

$$\boldsymbol{\tau}_{\text{int}} = \boldsymbol{\tau}_{\text{mot}} - \mathbf{M}_{\text{exo}}(\mathbf{q}_{\text{avg}})\ddot{\mathbf{q}}_{\text{avg}} + \mathbf{n}_{\text{exo}}(\mathbf{q}_{\text{avg}}, \dot{\mathbf{q}}_{\text{avg}}) \quad (20)$$

with \mathbf{M}_{exo} being the mass matrix capturing the inertia of the Lokomat exoskeleton and \mathbf{n}_{exo} subsuming the Gravitational, friction, and Coriolis torques of the exoskeleton.

EMG signals were band-pass filtered between 15 and 300 Hz, rectified, and cut into single strides triggered by the heel

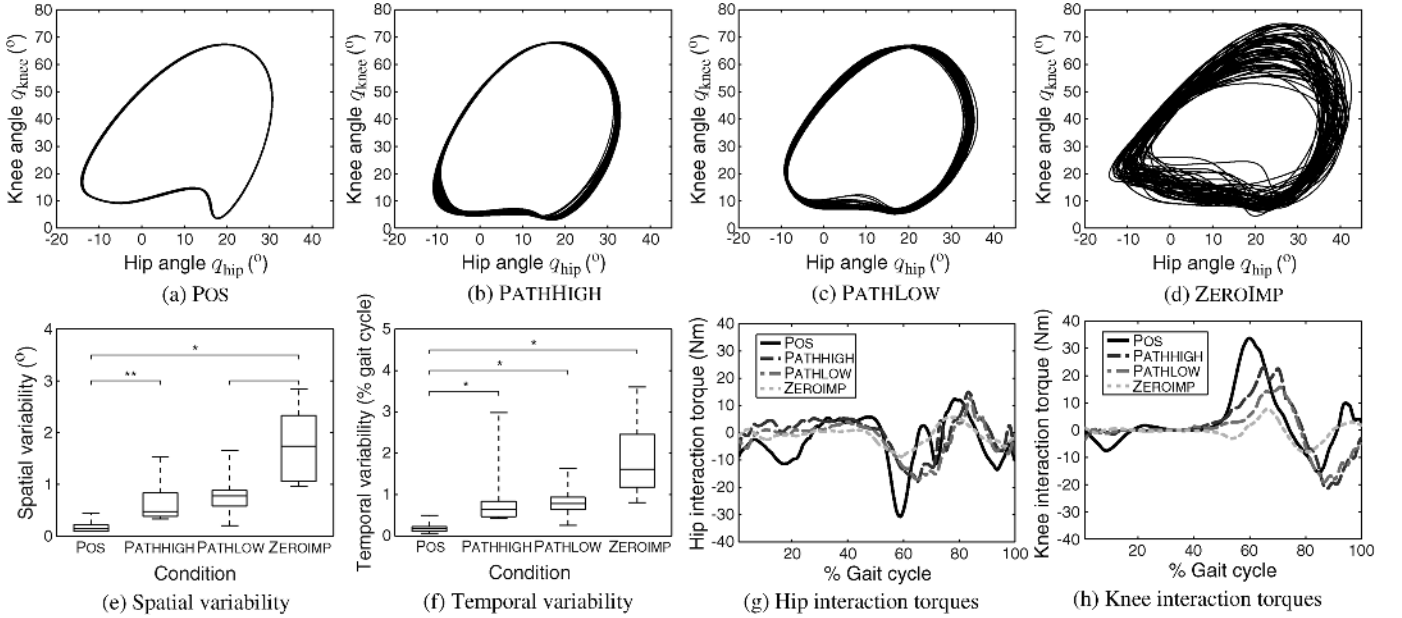


Fig. 4. Resulting kinematic and kinetic data. Trajectories in joint space for one exemplary healthy subject (female, 170 cm, 59 kg) under the different conditions POS (a), PATHHIGH (b), PATHLOW (c), ZEROIMP (d). Box plots of spatial variability var_ξ (e) and temporal variability var_τ (f) of healthy subjects. Hip (g) and knee (h) interaction torques τ_{int} computed according to (20) and averaged over healthy subjects ($n = 10$).

strike signal of the foot switches. The single strides were normalized in time to 1001 samples each. All strides of a subject under a given condition were then averaged. Next, the average strides were broken up into seven phases (initial loading, mid-stance, terminal stance, preswing, initial swing, midswing, terminal swing) according to Perry [31]. The root mean square (rms) of the EMG signals was calculated for each muscle within each of these phases.

The rms values of the EMG signals showed high inter-subject variability, and the repeated measurements for a single subject were not independent of each other. Linear mixed models [32] are a statistical tool that can account for such circumstances. In these models, random variables can capture the covariance of multiple data values originating from different individual sources. The remaining, subject-independent effects can be described as the linear influence of fixed factors.

To investigate the influence of the different conditions on muscle activity, we fitted a separate linear mixed model to the logarithm of the rms values of the EMG signals of each muscle. For a given muscle, we define the logarithmized rms for an observation j in a subject i as EMG_{ij} . An observation is a combination of one of the four conditions and one of the seven gait phases. Hence, there were $7 \times 4 = 28$ observations j ($j = 1, 2, \dots, 28$) per subject. We included the factors “condition” and “gait phase” as fixed effects. Thus, the value of EMG_{ij} for a given observation j on the i th subject was modeled as

$$\begin{aligned} \text{EMG}_{ij} = & \beta_0 + \beta_1 \times \text{COND1}_{ij} + \beta_2 \times \text{COND2}_{ij} \\ & + \beta_3 \times \text{COND3}_{ij} + \beta_4 \times \text{PHASE1}_{ij} \\ & + \beta_5 \times \text{PHASE2}_{ij} + \dots + \beta_9 \times \text{PHASE6}_{ij} \\ & + u_{0i} + \varepsilon_{ij}. \end{aligned} \quad (21)$$

The indicator variables COND1_{ij} to PHASE6_{ij} were set to one, if the observation j belonged to the respective condition

or gait phase, otherwise to zero. To account for the correlation of repeated measurements within a subject i , a random intercept u_{0i} was assumed for each subject. The residual ε_{ij} captures the difference between the measured value EMG_{ij} and the prediction of the model.

In order to compare the different conditions, we computed the estimated marginal means for each condition by averaging the model predictions across the different gait phases. These estimated marginal means were then compared with post-hoc tests at the 5% significance level. In these tests, multiple comparisons were accounted for by the Bonferroni adjustment. A similar statistical analysis of EMG data can be found in [33].

2) *Experiment With iSCI Subjects*: To assess how well subjects could walk with the path control strategy, the last 60 s of the timing error ΔS during walking under the path control condition were analyzed. The moving window limited the maximum of the timing error to 20% of the gait cycle. We considered subjects whose median timing error lay closer to 0 (perfect performance) than to the window border (worst possible performance) as “performing well.” Subjects whose median timing error lay closer to the window border than to 0 were considered as “performing with difficulties.” Healthy subjects were generally able to achieve “performing well” status when concentrating on the task in a pretrial.

III. RESULTS

A. Healthy Subjects

The results obtained under the condition PATHMEDIUM were always within the range between PATHLOW and PATHHIGH. However, due to the large amount of variation in the data, the evaluation of this condition does not contain additional information and is left out in the following sections for clarity of presentation. No noticeable asymmetries in the gait of the

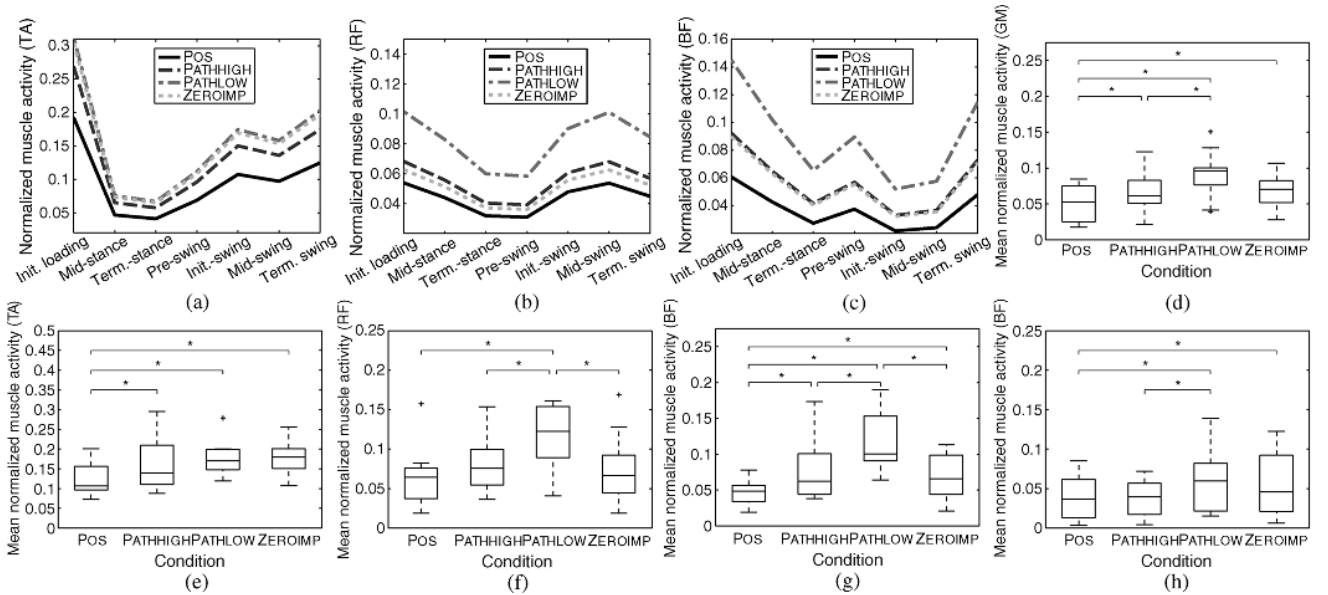


Fig. 5. Muscle activity of TA (Tibialis anterior), RF (Rectus femoris), and BF (Biceps femoris) muscles as predicted by the linear mixed models (a)–(c). Comparison of mean muscle activity for GM (Gastrocnemius medialis), TA, RF, BF, and VM (Vastus medialis) muscles (d)–(h). (a) Modeled TA activity; (b) modeled RF activity; (c) modeled BF activity; (d) comparison of GM activity; (e) comparison of TA activity; (f) comparison of RF activity; (g) comparison of BF activity; (h) comparison of VM activity.

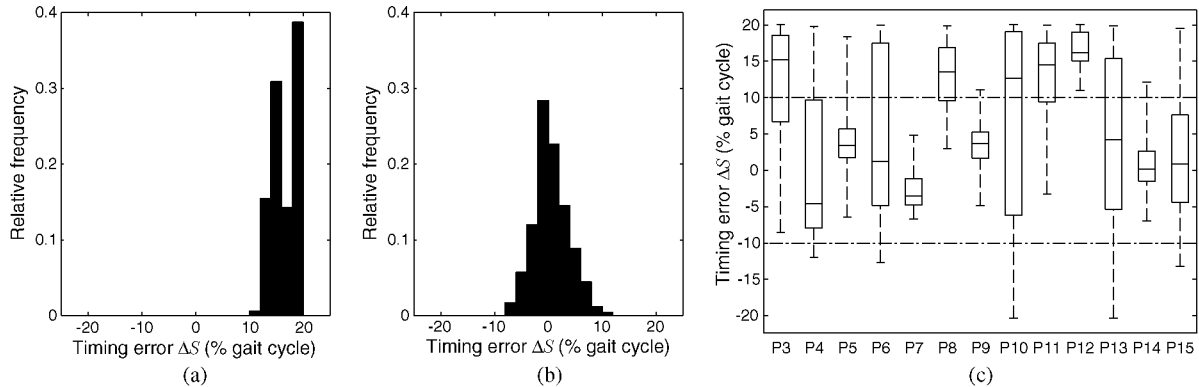


Fig. 6. Histograms of timing error $\Delta S(t)$ of two iSCI subjects and boxplot of timing errors of all iSCI subjects who were able to train with the path control strategy. Positive values indicate that the patient is lagging behind the desired movements; negative values indicate that the patient is moving too fast. (a) Timing error of iSCI subject P12; (b) timing error of iSCI subject P14; (c) timing errors of iSCI subjects.

subjects were observed. Hence, the data obtained for the left leg is considered as representative for both legs in the subsequent analysis.

1) *Kinematic and Kinetic Data*: Under the POS condition, subjects were forced by the robot to track the defined trajectory [Fig. 4(a)]. Under the PATHLOW and PATHHIGH conditions, the movements of the subjects were constrained to the virtual tunnel in joint space [Fig. 4(b) and (c)]. Subjects moved with large fluctuations under the ZEROIMP condition [Fig. 4(d)].

The spatial variability var_ξ was significantly different between POS and PATHHIGH, between PATHLOW and ZEROIMP, and between POS and ZEROIMP [Fig. 4(e)]. The temporal variability var_τ under the conditions PATHLOW, PATHHIGH, and ZEROIMP was significantly increased compared to POS [Fig. 4(f)]. There were no other significant differences between conditions.

The interaction torques between robot and subject were lowest under condition ZEROIMP, highest during condition POS and at intermediate values for conditions PATHLOW and PATHHIGH [Fig. 4(g) and (h)].

2) *Muscle Activity*: The linear mixed models could be successfully fitted to the EMG data of all muscles. The fixed effects “condition” and “gait phase” both contributed significantly to the models. The residuals ε_{ij} were normally distributed. Post-hoc comparisons between the different conditions showed several significant differences [Fig. 5(e)–(g)]. In all muscles, the activity under the PATHLOW condition was significantly higher than the activity under the POS condition. In RF and BF, the activity under the PATHLOW condition was additionally significantly higher than the activity under the ZEROIMP condition. In GM, VM, RF, and BF, the activity under the PATHHIGH condition was significantly reduced compared to the PATHLOW condition.

B. iSCI Subjects

All iSCI subjects were able to understand the training task. No subject showed any problems under the position control condition. Two subjects (P1 and P2) had minor difficulties to walk under the impedance control condition. The same two subjects

were not able to train successfully under the path control condition. All other subjects managed to get synchronized with the “ghost legs” and match the shown movements, both under the impedance control and the path control condition.

The analysis of the performance of the remaining subjects under the path control condition showed that five subjects had median timing errors which were closer to the back wall than to the center of the moving window [median above upper dashed-dotted line in Fig. 6(c)]. These subjects were classified as “performing with difficulties.” Subject P12 is an example for such a performance [Fig. 6(a)]. Eight subjects had median timing errors which were closer to the center of the moving window than to its walls [median between upper and lower dashed-dotted line in Fig. 6(c)]. These subjects were classified as “performing well”. The close to bell-shaped distribution of the timing error of P14 [Fig. 6(b)] illustrates this high level of performance, which matches the performance of healthy subjects. No subjects had median timing errors closer to the front wall of the moving window than to its center.

IV. DISCUSSION

A. Influence on the Timing of Movements

The path control strategy was designed to let patients influence the timing of their movements during robot assisted gait training. Moreover, we wanted to allow some flexibility in the spatial pattern of the movement, while assuring that movements would still be physiologically correct. Our first research question aimed at validating the successful implementation of this design: Does the path control strategy allow subjects to influence the timing of their movements?

We compared the spatio-temporal characteristics of gait patterns recorded under the different conditions. The POS condition served as a benchmark for a completely predetermined type of robotic training [Fig. 4(a)]. The ZEROIMP condition, on the other hand, served as a benchmark for a robotic training that allowed as much influence as possible [Fig. 4(d)]. It should be noted that under all tested conditions, subjects were instructed to imitate the movements of a reference presented to them by graphical feedback. Therefore, spatial and temporal variability are caused by movement errors the subjects made with respect to the task instructions. However, the possibility to make errors also implies the possibility to try correcting them, i.e., general influence on the spatial and temporal characteristics of the movements.

The temporal variability of subjects walking in path control mode was close to the temporal variability in zero impedance mode [Fig. 4(f)]. Thus, subjects experienced freedom of timing in path control mode which was close to the experience under the ZEROIMP condition. For the spatial variability, three distinct levels could be identified. As expected, only small spatial variability occurred under the POS condition. Large spatial variability occurred under the unconstrained ZEROIMP condition. Under both path control conditions, subjects showed medium spatial variability in their gait pattern [Fig. 4(f)]. This spatial variability was possible within the range of the virtual tunnel around the reference trajectory (Fig. 3).

These findings indicate that with our implementation of the path control strategy, subjects can influence the timing of their

movements. Spatial variability of movements is possible within a controllable range.

B. Active Participation

Increased activity of patients during training is a general goal of patient-cooperative control strategies [9]. Therefore, we investigated if training with the path control strategy causes subjects to participate more actively.

Generally, subjects walked with more activity of all recorded muscles in path control mode compared to position control mode (Fig. 5). More specifically, the subject-independent models of muscle activity reveal features in the activity patterns congruent with the findings of Hidler and Wall [6]. The RF muscle is unphysiologically activated during swing phase [Fig. 5(b)], and the BF muscle shows an unusual peak at preswing [Fig. 5(c)]. These features are conserved in zero impedance and path control mode. Hidler and Wall hypothesized that these alterations may be due to the restriction of movements to the sagittal plane in the Lokomat. To ensure foot clearance during swing phase, subjects exert excessive activity in muscles in the unrestricted degrees of freedom, as they cannot rely on pelvis and abduction movements. This hypothesis is supported by the fact that in RF and BF muscles, activity in path control mode was even higher than in zero impedance mode [Fig. 5(f) and (g)]. In path control mode, subjects had to actively follow the defined spatial reference which required exaggerated knee flexion (to prevent toes from catching on the treadmill). In zero-impedance mode, subjects could choose a more “energy-optimal” pattern that sacrificed some foot clearance for less excessive muscle contractions.

Thus, subjects participated more actively in path control mode, showing activity patterns consistent with those reported for walking restricted to the sagittal plane.

C. Modulation of Muscle Activity

We implemented supportive torques tangential to the desired movement path in joint space, which aimed at empowering subjects to move their legs with less effort, i.e., with less muscle activity. To understand the effects of this kind of support, we tried to modulate how actively subjects have to participate in the training by adjusting the support.

In all muscles except the TA, we observed a reduction of activity when the support was increased (Fig. 5). This means that the feed forward supportive torques τ_{sup} effectively reduced the effort of walking. The TA muscle, which is mainly active to induce ankle dorsiflexion is not modulated by the support, as the Lokomat does not actuate the ankle joint. Furthermore, the increased supportive torques particularly compensated the effect of the shape of the path (increased knee flexion during swing phase and pronounced knee extension at heel strike, cf. Section IV-B). The activity of the RF and BF muscles was reduced to the level of the zero impedance mode.

Thus, the level of active participation was successfully modulated by the supportive torques.

D. Feasibility of Training With iSCI Subjects

For the clinical relevance of the developed patient-cooperative controller, it is crucial whether iSCI subjects are able

to perform gait training with it. The evaluation with healthy subjects shows that the path control strategy provides the desired freedom of timing, and—within the borders of the virtual tunnel—also more influence on the spatial path of the movements. As a next step, we tested if iSCI subjects were able to move synchronously with a visual reference. If they managed to “perform well,” they were not pushed forward by the back wall of the moving window and, thus, autonomously controlling the timing of their leg movements. The size of the moving window ($\pm 20\%$ of the gait cycle) was chosen such that it was not possible to “accidentally perform well” by means of passive fluctuations in the moving window. Passive behavior resulted in fluctuations close to the back wall of the moving window, as seen in subjects P3, P8, P11, and P12. With a smaller window, similar but less distinct differences between the single subjects could be expected.

Thirteen out of 15 tested iSCI subjects were able to train with the path control strategy, eight of them performed well in the training task. No relations between training performance and Asia Impairment Scale, SCIM III mobility score, or WISCI II score were observed. It is striking that just the first two (P1 and P2) of all subjects were not able to train with the Path Control strategy, even though no changes to controller or protocol were made after these subjects. To rule out that this result was caused by a lack of routine of the therapist, subject P2 was retested at a later stage but was still not able to perform the training.

The two subjects that could not train with the path control strategy had very weak control over their extensor muscles. Hence, they were not able to induce sufficient knee extension at the end of swing phase to move along the desired path. It was not possible to compensate for this “local” weakness with the “global” support parameter k_{sup} . An automatic adaptation algorithm that identifies the individual deficits of a patient as implemented for the upper extremity by Wolbrecht *et al.* [34] could possibly enable these subjects to train with the path control strategy. Such an approach may also enable the five patients who did not perform well but rather relied on the back wall of the moving window to also progress into the middle area of the moving window where they could train with more freedom of timing.

Moreover, some iSCI subjects showed slacking behavior by completely relying on the help of the tunnel wall to keep their legs extended during stance phase. “Leaning” on the tunnel wall, they did not properly transfer their body weight to the other leg during double support stance phase. As soon as the virtual tunnel permitted them more knee flexion to initiate swing phase, they tended to “fall” into swing phase instead of starting to lift their foot from the ground. This problem may be caused because the path control strategy is limited to the sagittal plane with independent controllers for each leg. In future work, we will evaluate a path in higher dimensional space, involving both legs as well as additional degrees of freedom for movements of the pelvis. Such a path would guide patients through the weight transfer from one leg to the other. Subsequent studies will be performed to clarify if involving these additional degrees of freedom can prevent the observed slacking behavior or if further interventions like perturbations in support will be necessary to increase the activity of the subjects in these situations.

Despite these occasional difficulties, training with the path control strategy was feasible for 85% of the tested iSCI subjects.

E. Related Work

Banala *et al.* [13] implemented the virtual tunnel approach of Cai *et al.* [11] for their “Active Leg Exoskeleton” (ALEX). In a pilot study with two stroke survivors [35], subjects adapted their spatial movement path to the reference with the help of additional visual feedback. After 15 days of training, the subjects covered a larger range of motion and had increased their walking speeds on the treadmill.

Though developed independently, the implementation of the virtual tunnel of Banala *et al.* is similar to the implementation of our path control strategy. One difference between both approaches is the moving window that allows more fine-grained control over the amount of freedom in our path control strategy.

Furthermore, Banala *et al.* focus on controlling the foot position in Cartesian space, whereas we focus on the leg posture in joint space. We did not want to explicitly train subjects to modify their gait pattern. Instead, we aimed at providing a safe and supporting environment, where they could train on their own. Therefore, the tunnel width in our setup was much larger than in the experiments of Banala *et al.* [35], who used tunnel width settings of 1–2 cm. Our tunnel width settings (when transformed from joint space to Cartesian space) varied from about 5 mm during midstance, over 3 cm during swing phase to about 10 cm around heel strike.

The implementation of our set point generation algorithm (cf. Section II-B) is similar to the timing control algorithm for the PAM/POGO devices by Aoyagi *et al.* [19]. In fact, increasing the gain in Aoyagi’s timing control algorithm to enable it to change timing more rapidly and introducing an additional dead band around the reference trajectory would yield a path control algorithm for the PAM/POGO devices.

F. Limitations

It should be noted that a constant treadmill speed was used throughout the presented experiments. Thus, the temporal freedom of both the path control and the zero impedance mode were limited to swing phase. Nevertheless, a substantial increase in temporal variability could be detected. To increase patient interactivity during training, we will combine the path control strategy with approaches which adapt the treadmill speed according to the intention of subjects [15].

The constant treadmill speed was also the reason for implementing separate controllers for the single legs rather than coupling them directly. As the treadmill is controlling the propulsion of the stance leg, the swing leg would not be able to move with free timing if there was a close coupling. A narrow moving window can be used to couple the movements of the legs, as in [11]. However, in our experiments, the moving window was so large ($\pm 20\%$ of the gait cycle) that it only enforced coupling if subjects were moving close to its back wall, which was only true for the iSCI subjects who were rated as “performing with difficulties.” Here, a higher dimensional tunnel may allow more flexible coupling of the different degrees-of-freedom.

The fixed walking pattern that defines the spatial movement path may not be ideal for every patient. As in position-controlled

Lokomat training, the pattern can be adapted manually by the therapist. However, it is not guaranteed that a pattern close to the “healthy” pattern of an individual patient can be achieved. For hemi-paretic patients, it would be possible to derive a desired path for the affected leg from observing the unaffected leg, as proposed by Vallery *et al.* [16]. For iSCI patients, an adaptive reshaping of the path, similar to the approach by Jezernik *et al.* [7], may improve the applicability of the path control strategy.

V. CONCLUSION

We have implemented and evaluated a strategy for patient-cooperative robotic gait training. The strategy consists of a control algorithm, which provides free timing of leg movements, and a suitable training task with visual feedback. The subject can be optionally supported in the direction of desired movements. Furthermore, temporal freedom can be limited to a “moving window” that proceeds along the movement path.

Experiments with healthy subjects showed that they can successfully influence the timing of their movements, while the possible spatial variability is defined by the robot. Increased support resulted in reduced muscle activity. Healthy subjects trained more actively in the new strategy than in a noncooperative training mode. Further tests showed that training with the new strategy was feasible also for iSCI subjects.

Future research should investigate the effects of the path control strategy on patients more comprehensively. If these effects are similar to those on healthy subjects found in this study, a controlled clinical trial will be performed, which will assess whether the training with the path control strategy can actually improve rehabilitation outcome.

ACKNOWLEDGMENT

The authors would like to thank all subjects that participated in this study. The authors would also like to thank H. Vallery, M. Wirz, and Marc Bolliger for their support.

REFERENCES

- [1] K. J. Sullivan, D. A. Brown, T. Klassen, S. Mulroy, T. Ge, S. P. Azen, and C. J. Winstein, “Effects of task-specific locomotor and strength training in adults who were ambulatory after stroke: Results of the STEPS randomized clinical trial,” *Phys. Therapy*, vol. 87, no. 12, pp. 1580–1602, 2007.
- [2] B. Dobkin, H. Barbeau, D. Deforge, J. Ditunno, R. Elashoff, D. Apple, M. Basso, A. Behrman, S. Harkema, M. Saulino, and M. Scott, “The evolution of walking-related outcomes over the first 12 weeks of rehabilitation for incomplete traumatic spinal cord injury: The multicenter randomized Spinal Cord Injury Locomotor Trial,” *Neurorehabil. Neural Repair*, vol. 21, no. 1, pp. 25–35, 2007.
- [3] G. Colombo, M. Joerg, R. Schreiber, and V. Dietz, “Treadmill training of paraplegic patients using a robotic orthosis,” *J. Rehabil. Res. Dev.*, vol. 37, no. 6, pp. 693–700, 2000.
- [4] S. Hesse, D. Uhlenbrock, and T. Sarkodie-Gyan, “Gait pattern of severely disabled hemiparetic subjects on a new controlled gait trainer as compared to assisted treadmill walking with partial body weight support,” *Clin. Rehabil.*, vol. 13, no. 5, pp. 401–410, 1999.
- [5] J. F. Israel, D. D. Campbell, J. H. Kahn, and G. T. Hornby, “Metabolic costs and muscle activity patterns during robotic- and therapist-assisted treadmill walking in individuals with incomplete spinal cord injury,” *Phys. Therapy*, vol. 86, no. 11, pp. 1466–1478, 2006.
- [6] J. M. Hidler and A. E. Wall, “Alterations in muscle activation patterns during robotic-assisted walking,” *Clin. Biomech.*, vol. 20, no. 2, pp. 184–193, 2005.
- [7] S. Jezernik, G. Colombo, and M. Morari, “Automatic gait-pattern adaptation algorithms for rehabilitation with a 4-DOF robotic orthosis,” *IEEE Trans. Robot. Autom.*, vol. 20, no. 3, pp. 574–582, Jun. 2004.
- [8] J. L. Emken, J. E. Bobrow, and D. J. Reinkensmeyer, “Robotic movement training as an optimization problem: Designing a controller that assists only as needed,” in *Proc. IEEE 9th Int. Conf. Rehabil. Robot.*, Chicago, 2005, pp. 307–312.
- [9] R. Riener, L. Lünenburger, S. Jezernik, M. Anderschitz, G. Colombo, and V. Dietz, “Patient-cooperative strategies for robot-aided treadmill training: First experimental results,” *IEEE Trans. Neural Syst. Rehabil. Eng.*, vol. 13, no. 3, pp. 380–394, Sep. 2005.
- [10] D. J. Reinkensmeyer, D. Aoyagi, J. L. Emken, J. A. Galvez, W. Ichinose, G. Kerdanyan, S. Maneekobkunwong, K. Minakata, J. A. Nessler, R. Weber, R. R. Roy, R. de Leon, J. E. Bobrow, S. J. Harkema, and V. R. Edgerton, “Tools for understanding and optimizing robotic gait training,” *J. Rehabil. Res. Develop.*, vol. 43, no. 5, pp. 657–670, 2006.
- [11] L. L. Cai, A. J. Fong, C. K. Otoshi, Y. Liang, J. W. Burdick, R. R. Roy, and V. R. Edgerton, “Implications of assist-as-needed robotic step training after a complete spinal cord injury on intrinsic strategies of motor learning,” *J. Neurosci.*, vol. 26, no. 41, pp. 10 564–10 568, 2006.
- [12] J. von Zitzewitz, A. Duschau-Wicke, M. Wellner, L. Lünenburger, and R. Riener, “Path control: A new approach in patient-cooperative gait training with the rehabilitation robot lokomat,” in *Joint Meet. German, Austrian, Swiss Soc. Biomed. Eng.*, Zurich, 2006.
- [13] S. K. Banala, S. K. Agrawal, and J. P. Scholz, “Active Leg Exoskeleton (ALEX) for gait rehabilitation of motor-impaired patients,” in *Proc. IEEE 10th Int. Conf. Rehabil. Robot.*, Noordwijk, The Netherlands, 2007, pp. 401–407.
- [14] E. H. F. Van Asseldonk, R. Ekkelenkamp, J. F. Veneman, F. C. T. Van der Helm, and H. van der Kooij, “Selective control of a subtask of walking in a robotic gait trainer (LOPES),” in *Proc. IEEE 10th Int. Conf. Rehabil. Robot.*, 2007, pp. 841–848.
- [15] J. von Zitzewitz, M. Bernhardt, and R. Riener, “A novel method for automatic treadmill speed adaptation,” *IEEE Trans. Neural Syst. Rehabil. Eng.*, vol. 15, no. 3, pp. 401–409, Sep. 2007.
- [16] H. Vallery, E. van Asseldonk, M. Buss, and H. van der Kooij, “Reference trajectory generation for rehabilitation robots: Complementary limb motion estimation,” *IEEE Trans. Neural Syst. Rehabil. Eng.*, vol. 17, no. 1, pp. 23–30, Feb. 2009.
- [17] D. P. Ferris, K. E. Gordon, J. A. Beres-Jones, and S. J. Harkema, “Muscle activation during unilateral stepping occurs in the nonstepping limb of humans with clinically complete spinal cord injury,” *Spinal Cord*, vol. 42, no. 1, pp. 14–23, 2004.
- [18] M. Pohl, J. Mehrholz, C. Ritschel, and S. Ruckriem, “Speed-dependent treadmill training in ambulatory hemiparetic stroke patients: A randomized controlled trial,” *Stroke*, vol. 33, no. 2, pp. 553–558, 2002.
- [19] D. Aoyagi, W. E. Ichinose, S. J. Harkema, D. J. Reinkensmeyer, and J. E. Bobrow, “A robot and control algorithm that can synchronously assist in naturalistic motion during body-weight-supported gait training following neurologic injury,” *IEEE Trans. Neural Syst. Rehabil. Eng.*, vol. 15, no. 3, pp. 387–400, Sep. 2007.
- [20] J. F. Veneman, R. Kruidhof, E. E. G. Hekman, R. Ekkelenkamp, E. H. F. Van Asseldonk, and H. van der Kooij, “Design and evaluation of the LOPES exoskeleton robot for interactive gait rehabilitation,” *IEEE Trans. Neural Syst. Rehabil. Eng.*, vol. 15, no. 3, pp. 379–386, Sep. 2007.
- [21] H. Krebs, J. J. Palazzolo, L. Dipietro, M. Ferraro, J. Krol, K. Ranekleiv, Volpe, and N. Hogan, “Rehabilitation robotics: Performance-based progressive robot-assisted therapy,” *Autonomous Robots*, vol. 15, no. 1, pp. 7–20, 2003.
- [22] A. Duschau-Wicke, J. von Zitzewitz, R. Banz, and R. Riener, “Iterative learning synchronization of robotic rehabilitation tasks,” in *Proc. IEEE 10th Int. Conf. Rehabil. Robot.*, 2007, pp. 335–340.
- [23] T. Koritnik, T. Bajd, and M. Muih, “Virtual environment for lower-extremities training,” *Gait Posture*, vol. 27, no. 2, pp. 323–330, 2007.
- [24] H. J. Hermens, B. Freriks, R. Merletti, D. Stegeman, J. Blok, G. Rau, C. Disselhorst-Klug, and G. Haegg, European recommendations for surface electromyography 1999.
- [25] F. M. Maynard, M. B. Bracken, G. Creasey, J. F. Ditunno, W. H. Donovan, T. B. Ducker, S. L. Garber, R. J. Marino, S. L. Stover, and C. H. Tator, “International standards for neurological and functional classification of spinal cord injury,” *Spinal Cord*, vol. 35, pp. 266–274, 1997, Others.

- [26] M. Itzkovich, I. Gelernter, F. Biering-Sorensen, C. Weeks, M. T. Laramee, B. C. Craven, M. Tonack, S. L. Hitzig, E. Glaser, G. Zeilig, S. Aito, G. Scivoletto, M. Mecci, R. J. Chadwick, W. S. Masry, A. Osman, C. A. Glass, P. Silva, B. M. Soni, B. P. Gardner, G. Savic, E. M. Bergström, V. Bluvshstein, J. Ronen, and A. Catz, "The Spinal Cord Independence Measure (SCIM) version III: Reliability and validity in a multi-center international study," *Disabil. Rehabil.*, vol. 29, no. 24, pp. 1926–1933, 2007.
- [27] P. L. Dittuno and J. F. Dittuno, "Walking index for spinal cord injury (WISCI II): Scale revision," *Spinal Cord*, vol. 39, pp. 654–656, 2001.
- [28] W. Ilg, R. Rörig, P. Thier, and M. A. Giese, "Learning-based methods for the analysis of intralimb-coordination and adaptation of locomotor patterns in cerebellar patients," in *Proc. IEEE 10th Int. Conf. Rehabil. Robot.*, Noordwijk, The Netherlands, 2007, pp. 1090–1095.
- [29] M. A. Giese and T. Poggio, "Morphable models for the analysis and synthesis of complex motion patterns," *Int. J. Comp. Vis.*, vol. 38, no. 1, pp. 59–73, 2000.
- [30] J. D. Gibbons, *Nonparametric Statistical Inference*. New York: Marcel Dekker, 1985.
- [31] J. Perry, *Gait Analysis: Normal and Pathological Function*. Thorofare, NJ: SLACK, 1992.
- [32] B. T. West, K. B. Welch, and A. T. Galecki, *Linear Mixed Models: A Practical Guide Using Statistical Software*. New York: Chapman Hall/CRC Press, 2006.
- [33] E. H. F. van Asseldonk, J. F. Veneman, R. Ekkelenkamp, J. H. Buurke, F. C. T. van der Helm, and H. van der Kooij, "The effects on kinematics and muscle activity of walking in a robotic gait trainer during zero-force control," *IEEE Trans. Neural Syst. Rehabil. Eng.*, vol. 16, no. 4, pp. 360–370, Aug. 2008.
- [34] E. T. Wolbrecht, V. Chan, D. J. Reinkensmeyer, and J. E. Bobrow, "Optimizing compliant, model-based robotic assistance to promote neurorehabilitation," *IEEE Trans. Neural Syst. Rehabil. Eng.*, vol. 16, no. 3, pp. 286–297, Jun. 2008.
- [35] S. K. Banala, S. H. Kim, S. K. Agrawal, and J. P. Scholz, "Robot assisted gait training with Active Leg Exoskeleton (ALEX)," *IEEE Trans. Neural Syst. Rehabil. Eng.*, vol. 17, no. 1, pp. 2–8, Feb. 2009.



Alexander Duschau-Wicke (S'09) was born in Bochum, Germany, in 1980. From 2000 to 2005, he studied Electrical and Computer Engineering at TU Kaiserslautern, Germany, and University of Michigan, Ann Arbor. The main focuses of his studies were control systems, automatic control, and medical technology. After receiving the Dipl.-Ing. degree from TU Kaiserslautern, he started his doctorate studies in a collaboration project between the medical engineering company Hocoma AG (Volketswil, Switzerland) and ETH Zurich.

His research interests are centered on the development of new patient-cooperative control strategies for robot-aided gait rehabilitation.



Joachim von Zitzewitz (S'09) received the M.Sc. degree (honors) in mechanical engineering from the Graz University of Technology, Graz, Austria, in 2006. He is currently finishing his Ph.D. theses at the Sensory-Motor Systems Lab, ETH Zurich, Switzerland, where he focuses on reconfigurable, tendon-based haptic interfaces. I

n 2005, he worked at the Automatic Control Laboratory, ETH Zurich, Switzerland, concentrating on patient-cooperative control strategies for rehabilitation robots. His research interests include

human-machine interfaces as well as parallel manipulators.



Andrea Caprez received the M.Sc. degree in human movement sciences from the Institute for Biomechanics at the Swiss Federal Institute of Technology (ETH), Zurich, Switzerland, in 2008. Her M.S. thesis focuses on robotic patient-cooperative gait training.

In 2007 she joined ETHs Sensory-Motor Systems Lab, where she worked on robotic, patient-cooperative gait training with spinal cord injured patients in collaboration with the Spinal Cord Injury Center at Balgrist University Hospital, Zurich, Switzerland. Since 2008 she has been working as a sport therapist at the Schulthess Clinic Swiss Olympic Medical Center, Zurich, Switzerland.



Lars Lünenburger (M'05) was born in Siegen, Germany, in 1972. He studied physics and mathematics in Siegen, Germany and Zurich, Switzerland. He received the Dipl. Phys. ETH degree from the Swiss Federal Institute of Technology, Zurich, Switzerland, in 1997, and the Dr. rer. nat. degree from the Faculty of Biology at Bochum University, Bochum, Germany, for his doctoral thesis work on the neuronal basis of eye-hand coordination, in 2002.

From 2002 to 2006, he was with the Research Laboratory, Spinal Cord Injury Center, Balgrist University Hospital, Zurich, Switzerland. Since 2006, he is with Hocoma AG, Volketswil, Switzerland, that develops and produces rehabilitation devices. He is Head of Software Engineering and product manager for Augmented Feedback. His research interests are the development, application, and use of robotic rehabilitation devices for training and assessment of patients.

Dr. Lünenburger is a member of the Neural Control of Movement (NCM) Society.



Robert Riener (M'95) received the Ph.D. degree from TU München in 1997. After postdoctoral work at the Politecnico di Milano, he completed his Habilitation in the field of Biomechanics at TU München in 2003.

From 2003 to 2006 he was Assistant Professor of Rehabilitation Engineering at ETH Zurich and SCI Center, University Hospital Balgrist. Since June 2006, he has been Associate Professor for Sensory-Motor Systems while holding his double affiliation at ETH and Balgrist. His research interests include neuroprosthetics, haptics, and rehabilitation robotics. He has authored more than 250 peer-reviewed articles and 18 patents.

Dr. Riener is an Associate Editor of the IEEE TRANSACTIONS ON NEURAL SYSTEMS AND REHABILITATION ENGINEERING and other international journals. Since 2008 is the Head of the Institute of Robotics and Intelligent Systems (IRIS) at ETH Zurich.